Enhancing mechanical properties via adding Ni and Zn in Cu/Sn3.5Ag/Cu transient liquid phase bonding for advanced electronic packaging

Zih-You Wu[1], Tzu-Chia Wang[1], Yu-Ching Wang[1], Rui-Wen Song[1], Su-Yueh Tsai[2], and Jenq-Gong Duh[1,3,*]

[1] *Department of Materials Science and Engineering, National Tsing Hua University, Hsinchu, Taiwan*
[2] *Precision Instrument Center, National Tsing Hua University, Hsinchu, Taiwan*
[3] *No. 101, Sec. 2, Kuang-Fu Road, Hsinchu 30013, Taiwan*

ABSTRACT

Recently, the transient liquid phase (TLP) bonding process has become a promising method in advanced electronic packaging. Full intermetallic compounds joints provide good strength and reliable high-melting-point phase after bonding. However, Kirkendall voids and the preferred orientation of Cu_6Sn_5 may deteriorate the reliability in conventional Cu/Sn/Cu bumps. To resolve these problems and further enhance the mechanical proprieties, Ni and Zn are used to modify the overall microstructures of the TLP bond. After the addition of Ni and Zn, the strength of Cu18Ni/Sn3.5Ag/Cu and Cu18Ni18Zn/Sn3.5Ag/Cu bump increased significantly, as compared to Cu/Sn3.5Ag/Cu. Both Cu18Ni/Sn3.5Ag/Cu and Cu18Ni18Zn/Sn3.5Ag/Cu bump demonstrated outstanding strength and toughness. Moreover, microstructure, grain, and mechanical analyses are employed to elucidate the mechanisms behind the strengthening effect of Ni and Zn in Cu18Ni/Sn3.5Ag/Cu and Cu18Ni18Zn/Sn3.5Ag/Cu bump.

1 Introduction

In advanced electronic packaging, the density of input/output connections will increase and the bump sizes become smaller. In the microbump generation, the sizes might be scaled down to smaller than 10 μm in the near future. The fraction of the intermetallic compounds (IMCs) plays a critical role in the reliability of electronic products in such a small volume of solder [1, 2]. Therefore, the transient liquid phase (TLP) soldering was developed to be a potential bonding method for advanced packaging because of the following reasons. Firstly, TLP bonding can produce reliable and high melting point joints due to the formation of full IMCs after bonding [3, 4]. Thus, the joints can endure elevated temperature process in consecutive reflow and can be used in high-temperature power devices. Furthermore, the mechanical

---

Address correspondence to E-mail: jgd@mx.nthu.edu.tw

properties of the microbump would increase evidently as full IMCs form, and the fracture mode is dominated by the characteristic of IMCs since there is no solder left over [5]. Consequently, it is critical to realize the mechanical properties of the IMCs and the fracture mechanism.

In traditional Cu/Sn/Cu system, two main problems significantly deteriorate the reliability of TLP microbump. One of the issues is that upper and bottom Cu_6Sn_5 typically become one single grain per column during TLP bonding [4, 6]. The other is the strong preferred orientation of Cu_6Sn_5 along c-axis, which is parallel to the IMC growth direction [7, 8]. Such issues mentioned above may result in easy crack propagation when joints suffered stress concentration. Moreover, the formation of Kirkendall voids accompanied by Cu_3Sn layer was also a challenge to be tackled. In previous studies, Ni and Zn-doped substrate has shown the potential to suppress the growth of Cu_3Sn layer and thus inhibit the Kirkendall voids formation [9, 10]. Besides, the solute atoms acting as nucleation sites might refine the grain size and diversify the grain orientations. The microstructural enhancement of micro-joints could upgrade the reliability. These improvements are expected to enhance the mechanical properties and prolong the product life.

2 Experimental procedure

Three conditions of microbumps were discussed in this research, including Cu/Sn3.5Ag/Cu, Cu18Ni/Sn3.5Ag/Cu, and Cu18Ni18Zn/Sn3.5Ag/Cu. The Cu and Cu18Ni18Zn substrates were acquired from commercial C1100 and C7521 alloy, respectively. The Cu18Ni substrate was fabricated by co-sputtering Cu and Ni targets on Cu substrates, and the thickness of the film was about 2.5 μm. The compositions of Cu18Ni and Cu18Ni18Zn substrates were confirmed by quantitative analysis in field emission electron probe micro-analyzer (FE-EPMA; IHP-200 F, JEOL). The upper boards were $2 \times 2 \times 0.3$ mm^3, while the bottom boards were $2 \times 10 \times 1$ mm^3 for shear test. Appropriate grinding and acidic dipping process were used to obtain clean substrate surfaces. The Sn-3.5Ag solder balls with 1 mg were then placed between two substrates. They were stacked into a sandwich structure and subjected to reflow at a peak temperature of 260 °C for 300 s, and a bonding

pressure of 1.6 MPa was applied during reflow. The water-soluble flux was used to remove the oxidation and contamination during heating. Afterward, all the solder joints were air-cooled to room temperature and the bump height was around 5 μm.

The samples for microstructural observation were cold-mounted in the epoxy resin and were ground with sandpapers. To further acquire high-quality analyzing surface, cross section polisher with ion milling function was also utilized for surface cleaning. Other samples for mechanical tests were conducted by a shear tester (Condor Sigma, Xyztec). The shear speed was 500 μm/s and shear height was 30 μm. The cross-sectional images of as-bonded samples and fracture samples were observed by field emission scanning electron microscopy (FE-SEM; JSM-7600 F, JEOL). Electron backscatter diffraction (EBSD) analysis was used to acquire the information of grain sizes and the growth orientation. Moreover, the elemental distribution and the composition of IMC phases in micro-joints were measured by FE-EPMA.

3 Results and discussion

3.1 Microstructure and elemental analysis

Figure 1 demonstrates the back-scattered electron images of the Cu/Sn3.5Ag/Cu, Cu18Ni/Sn3.5Ag/Cu, and Cu18Ni18Zn/Sn3.5Ag/Cu cross section. It is already a full intermetallic compound structure with no residual Sn solder existed. In Cu/Sn3.5Ag/Cu bump, the layer-type Cu_3Sn was observed in both interfaces between substrates and Cu_6Sn_5. However, the Cu_3Sn layer was only seen near the Cu board in Cu18Ni/Sn3.5Ag/Cu and Cu18Ni18Zn/Sn3.5Ag/Cu. The Cu_3Sn layer was effectively eliminated near the top board with element addition. Both Ni and Zn were shown to suppress the growth of Cu_3Sn in previous literatures [3, 11]. The Cu_3Sn growth was partially retarded due to the Ni effect in Cu18Ni/Sn3.5Ag/Cu. Nevertheless, with the Ni and Zn combined, the Cu_3Sn layer almost disappeared in Cu18Ni18Zn/Sn3.5Ag/Cu, and only the discontinuous layer was barely seen in Fig. 1c. As the formation of Kirkendall voids and the smooth phase boundaries between Cu_6Sn_5 and Cu_3Sn would lead to cracks initiation and easy propagation [3], the suppression of Cu_3Sn is expected to diminish the weak points in
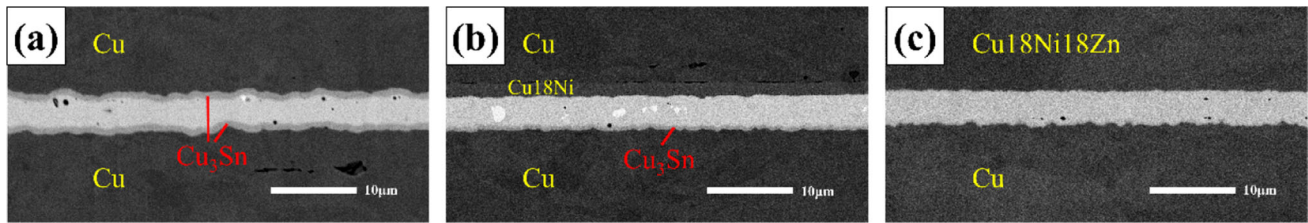
Fig. 1 Back-scattered electron images of **a** Cu/Sn3.5Ag/Cu **b** Cu18Ni/Sn3.5Ag/Cu **c** Cu18Ni18Zn/Sn3.5Ag/Cu reflowed at 260 °C for 300 s

the joint. In addition, Ni and Zn could stabilize the high temperature phase of Cu_6Sn_5, which inhibit phase transformation into low temperature phase [12–14]. It was reported that the polymorphic phase transformation of Cu_6Sn_5 would result in volume expansion and residual stress in IMCs, further leading to crack initiation [15]. Therefore, the stabilization of the Cu_6Sn_5 phase by Ni and Zn is a favorable modification for improving joints performance.

The elemental color mapping of Cu18Ni/Sn3.5Ag/Cu and Cu18Ni18Zn/Sn3.5Ag/Cu is revealed in Fig. 2. A Cu18Ni layer on the top of the Cu18Ni/Sn3.5Ag/Cu was confirmed to supply sufficient Ni contents during reflowing process through Ni mapping. The concentration of Ni in Cu18Ni/Sn3.5Ag/Cu and Cu18Ni18Zn/Sn3.5Ag/Cu was uniform throughout the microbump except for thin Ni-rich area along upper interfaces, which were corresponded to tiny grains as shown in Fig. 3b and c. Comparatively, the distribution of Zn atoms was homogeneously distributed in Cu_6Sn_5 grains. The dissolution of Ni decreased the Cu solubility in Sn, leading to nodule-like Cu_6Sn_5 participate [16]. Furthermore, simultaneous co-existence of both Ni and Zn could accelerate the growth rate of IMCs after reflow [13], inducing shortened time to form full TLP bonding. In order to confirm the composition of Cu_6Sn_5, the quantitative analyses were utilized as listed in Table 1. In Cu18Ni/Sn3.5Ag/Cu microbump, Cu atoms in Cu_6Sn_5 were replaced by Ni to form $(Cu,Ni)_6Sn_5$. As for Cu18Ni18Zn/Sn3.5Ag/Cu microbump, the solute Ni and Zn atoms substituted the Cu and Sn atoms to form $(Cu,Ni)_6(Sn,Zn)_5$, respectively [13]. The concentration of Ni increased from 3.08 to 4.94 at.% when Zn was doped into solder. In other words, the Zn solute atoms could promote the dissolution of Ni solute atoms. In literatures, Young's modulus and hardness of Cu_6Sn_5 could be reinforced with increasing of Ni and Zn concentration due to solid solution strengthening [7, 17, 18].

This implied that $(Cu,Ni)_6(Sn,Zn)_5$ in Cu18Ni18Zn/Sn3.5Ag/Cu might demonstrate superior intrinsic properties than $(Cu,Ni)_6Sn_5$ in Cu18Ni/Sn3.5Ag/Cu.

3.2 Grain sizes and grain orientations

To realize more detailed grains information, the electron backscatter diffraction (EBSD) technique was applied to analyze grain sizes and growth orientations. As indicated by the TD arrow in Fig. 3d, the orientation maps were analyzed from the transverse direction (TD). Figure 3a illustrates the strongly preferred orientation of Cu_6Sn_5 in Cu/Sn3.5Ag/Cu, and a series of columnar grains are observed evidently from orientation map of Cu_6Sn_5. It is considered as the weak point in microbump, since crack propagation between adjacent crystal planes would easily occur without too much obstruction [19]. As shown in Fig. 3b, the grain sizes in Cu18Ni/Sn3.5Ag/Cu were clearly refined, especially along upper interface where corresponded to unidentified area nearby top substrate. The circumstance in Cu18Ni18Zn/Sn3.5Ag/Cu was similar to Cu18Ni/Sn3.5Ag/Cu. The Ni and Zn addition could act as nucleation sites for IMCs, leading to appreciable formation of refined grains [20]. Small grains growing from upper substrate exhibited high Ni contents and demonstrated random orientation. In contrast, IMCs growing from bottom substrate remained relatively intensely preferred orientation. Thus, Cu_6Sn_5 with strongly preferred orientation are considered as the easy paths for crack propagation. However, the tiny $(Cu,Ni)_6Sn_5$ and $(Cu,Ni)_6(Sn,Zn)_5$ grains near the top board were retained rather than being merged by the opposing grains. It is due to the fact that solute atoms, especially Sn and Zn, can distort the crystal structure of Cu_6Sn_5 owing to the discrepancy of atomic radius [4, 7]. The increasing concentration of solute atoms might bring about appreciable distortion of lattice structure. Moreover, Cu18Ni18Zn/Sn3.5Ag/Cu can
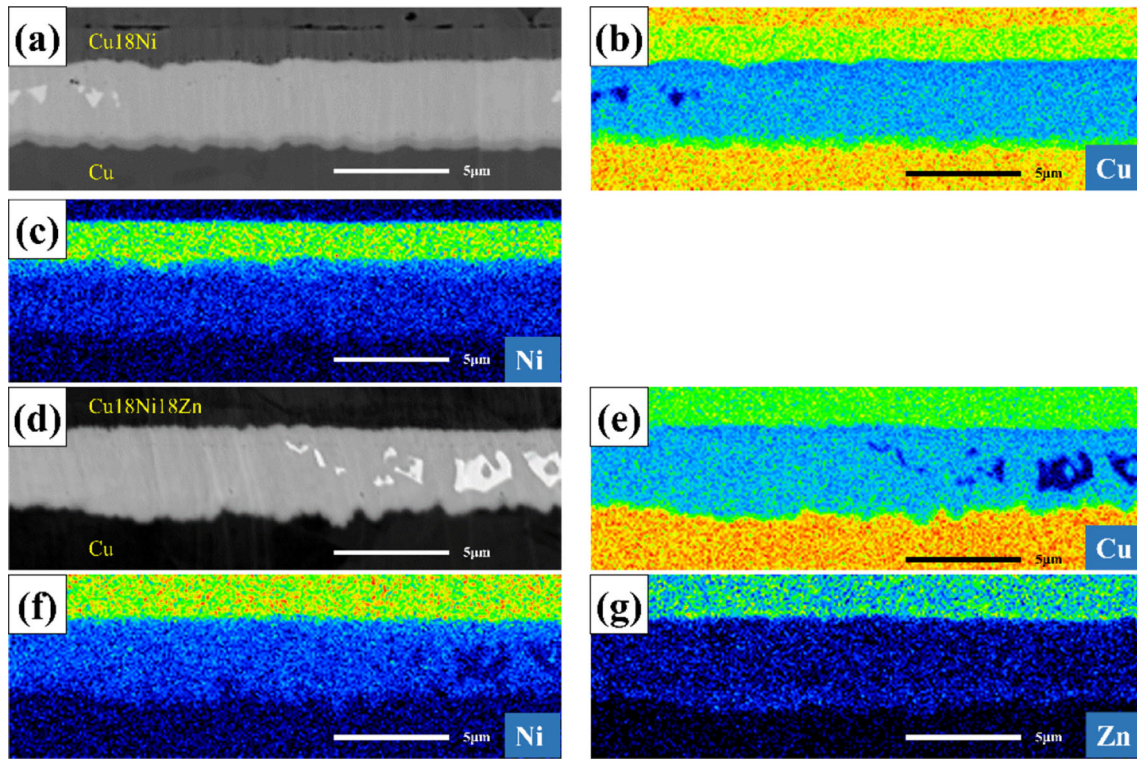
Fig. 2 FE-EPMA X-ray mapping images of Cu18Ni/Sn3.5Ag/Cu **a** back-scattered electron image, **b** Cu element, **c** Ni element and Cu18Ni18Zn/Sn3.5Ag/Cu **d** back-scattered electron image **e** Cu element **f** Ni element **g** Zn element
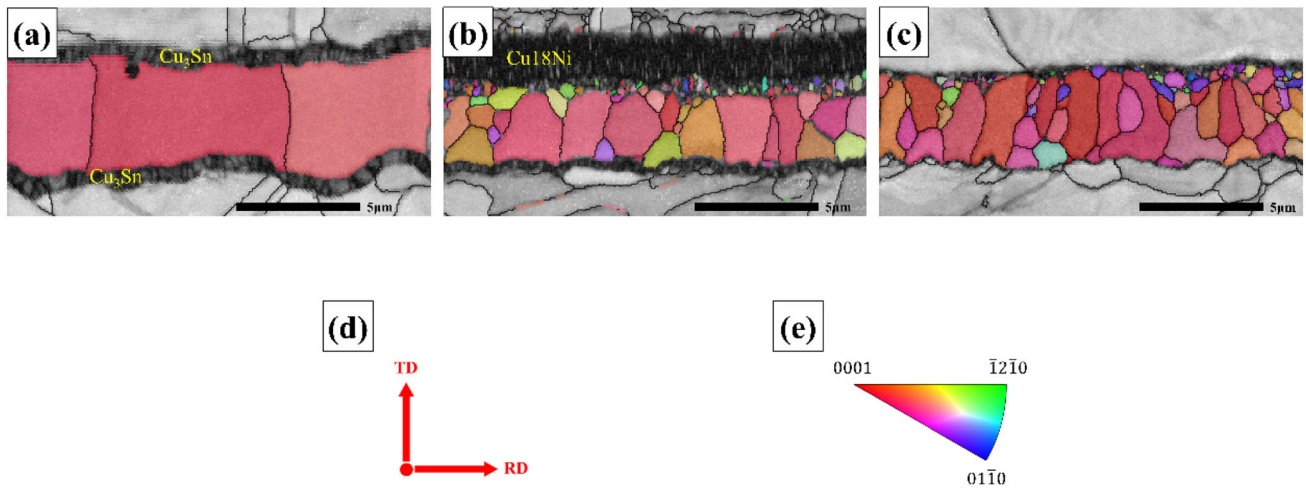
Fig. 3 EBSD orientation maps (TD) of **a** Cu/Sn3.5Ag/Cu, **b** Cu18Ni/Sn3.5Ag/Cu, **c** Cu18Ni18Zn/Sn3.5Ag/Cu, **d** the direction of TD, ND, and RD in EBSD analysis, and **e** the inverse pole figure of the TD direction

Table 1 Elemental quantification by FE-EPMA

	Cu (at.%)	Ag	Sn	Ni	Zn	Phase
Cu/SA/Cu	56.34	0.23	43.43	–	–	Cu_6Sn_5
Cu18Ni/SA/Cu	54.11	0.31	42.50	3.08	–	$(Cu,Ni)_6Sn_5$
Cu18Ni18Zn/SA/Cu	51.24	0.30	40.14	4.94	3.38	$(Cu,Ni)_6(Sn,Zn)_5$

reach full TLP bonding in shortened time, reducing the time and space for IMC to merge into columnar grains, and exhibit the finest grain structure. Consequently, the retaining phenomenon of IMCs from both substrates was clarified.

From the pole figure in Fig. 4a, it is revealed that the distribution of Cu_6Sn_5 in Cu/Sn3.5Ag/Cu was quite centralized along y-axis, and can also be an evidence for strongly (0001) preferred orientation. Nevertheless, the orientation of Cu_6Sn_5 becomes more random in Cu18Ni/Sn3.5Ag/Cu and Cu18Ni18Zn/Sn3.5Ag/Cu after Ni and Zn addition. Grain diversification is considered to be an enhancing phenomenon for hindering direct stress propagation to adjacent crystal planes [21]. Besides, the fine grains possess more fraction of grain boundary area, resulting in the improvement of hardness and yield strength according to grain boundary strengthening mechanism [3]. In combination with the effects of grain refinement and orientation diversification, the reliability of the microbump were enhanced.

## 3.3 Mechanical properties and fracture analysis

Shear tests were carried out on three conditions of microjoints formed by TLP soldering as shown in Fig. 5. 20 samples were tested and the average values were calculated for each condition. After collecting statistics, the average peak force of Cu18Ni/Sn3.5Ag/Cu was 62.33 MPa, which was increased by 43.16%, as compared to that of Cu/Sn3.5Ag/Cu for only 43.54 MPa. Furthermore, the average peak force was 82.79 MPa in Cu18Ni18Zn/Sn3.5Ag/Cu and it was increased by 90.15%, as compared to Cu/Sn3.5Ag/Cu. In general, strength is proportional to hardness. From others researches, the intrinsic improvement of Cu_6Sn_5 hardness and strength by adding Ni or Zn were characterized. As compared to Cu_6Sn_5, hardness of $(Cu,Ni)_6Sn_5$ increased 1.45% [22] and fracture strength increased 13.63% [17] via nanoindentation and micropillar compression testing, respectively. In addition, $Cu_6(Sn,Zn)_5$ increased 7.42% [23] or 3.04% [24] in hardness. The data above could not explain the 43.16 and 90.15% increasing of peak force with intrinsic improvement of Cu_6Sn_5. Thus, the strength enhancement would be mainly attributed to grain refinement and orientation diversification. This reveals that the ability to resist external shear force in Cu/Sn3.5Ag/Cu is improved by both Ni and Zn addition specifically. Moreover, the end energy in Cu18Ni18Zn/Sn3.5Ag/Cu and Cu18Ni/Sn3.5Ag/Cu is significantly greater than Cu/Sn3.5Ag/Cu. It means that Cu18Ni/Sn3.5Ag/Cu and Cu18Ni18Zn/Sn3.5Ag/Cu tended to provide better energy absorption capacity to withstand external stress and exhibit superior fracture toughness than Cu/Sn3.5Ag/Cu [9, 25]. Overall, both the toughness and shear strength are enhanced by doping Ni and Zn, and the mechanical performances of Cu18Ni18Zn/Sn3.5Ag/Cu are the most favorable among three cases.

After shear tests, cross section views of fracture samples were employed to reveal the crack paths. Investigating the crack path is necessary to further understand the weak points in microbumps. In conventional Cu/Sn/Cu TLP bumps, the large Cu_6Sn_5 grain with preferred orientation along (0001) direction and the smooth phase boundaries between Cu_6Sn_5 and Cu_3Sn are the weak points in microjoints [4, 5]. As shown in Fig. 6, the propagation path of cracks in Cu/Sn3.5Ag/Cu were divided into two
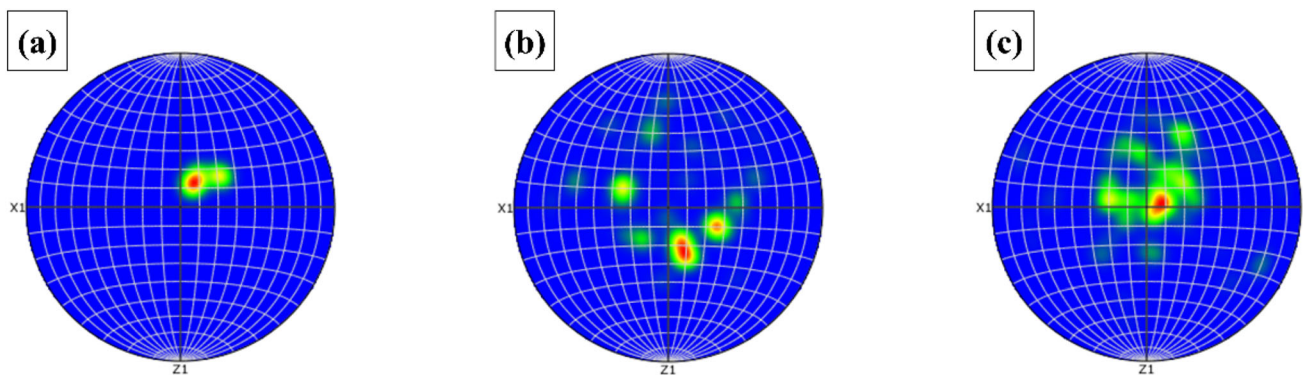
Fig. 4 Cu_6Sn_5 (0001) pole figure of **a** Cu/Sn3.5Ag/Cu **b** Cu18Ni/Sn3.5Ag/Cu **c** Cu18Ni18Zn/Sn3.5Ag/Cu
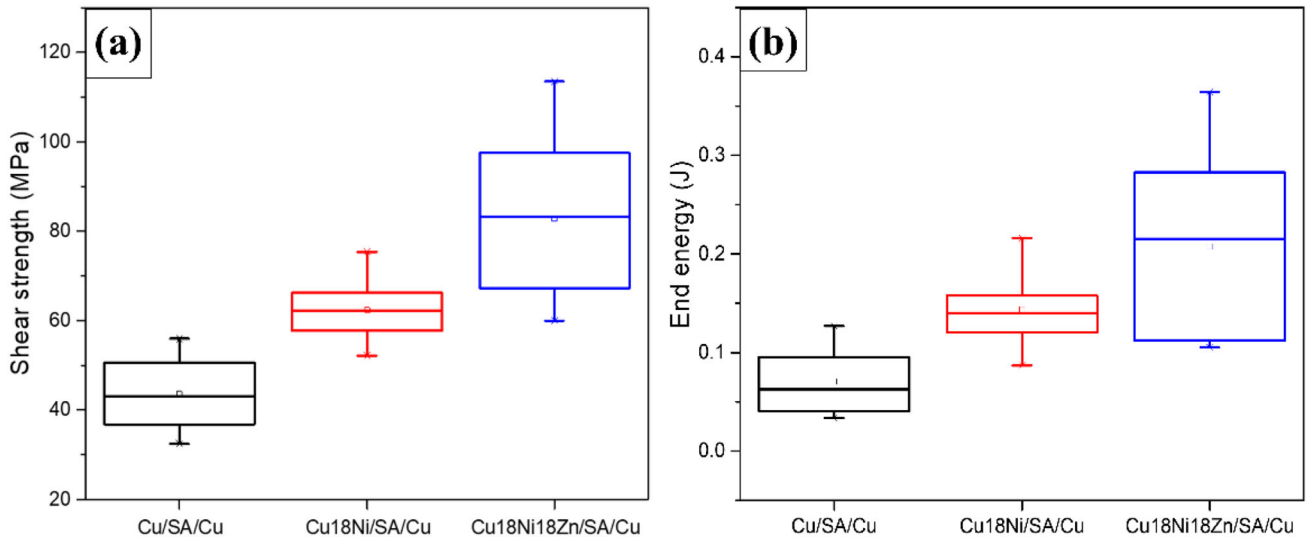
Fig. 5 The **a** shear strength and **b** end energy of Cu/Sn3.5Ag/Cu, Cu18Ni/Sn3.5Ag/Cu, and Cu18Ni18Zn/Sn3.5Ag/Cu

categories. One is going through Cu_6Sn_5 grains by cleavage [26]. The other is passing through the interface between Cu_6Sn_5 and Cu_3Sn layer [5]. After Ni and Zn addition, the Cu_6Sn_5 grains were refined and a large number of grain boundaries areas was induced. Thus, the crack propagation could be hindered [19]. As illustrated in Fig. 6b and c, the fracture morphologies of Cu18Ni/Sn3.5Ag/Cu and Cu18Ni18Zn/Sn3.5Ag/Cu were rough. Rougher

fracture surface means that the crack propagation in microjoints was more blocked [27]. The cracks might partially go through the grains while others propagate along the grain boundaries. It represented that the enhancement of intrinsic grain properties transferred the weak point into grain boundaries partly. In addition, the thickness of Cu_3Sn was retarded so that the smooth phase boundaries between Cu_6Sn_5 and Cu_3Sn in microjoints was mostly eliminated. When a

Fig. 6 The cross section images of **a** Cu/Sn3.5Ag/Cu **b** Cu18Ni/Sn3.5Ag/Cu **c** Cu18Ni18Zn/Sn3.5Ag/Cu and schematic illustration for fracture mechanism of **d** Cu/Sn3.5Ag/Cu **e** Cu18Ni/Sn3.5Ag/Cu **f** Cu18Ni18Zn/Sn3.5Ag/Cu
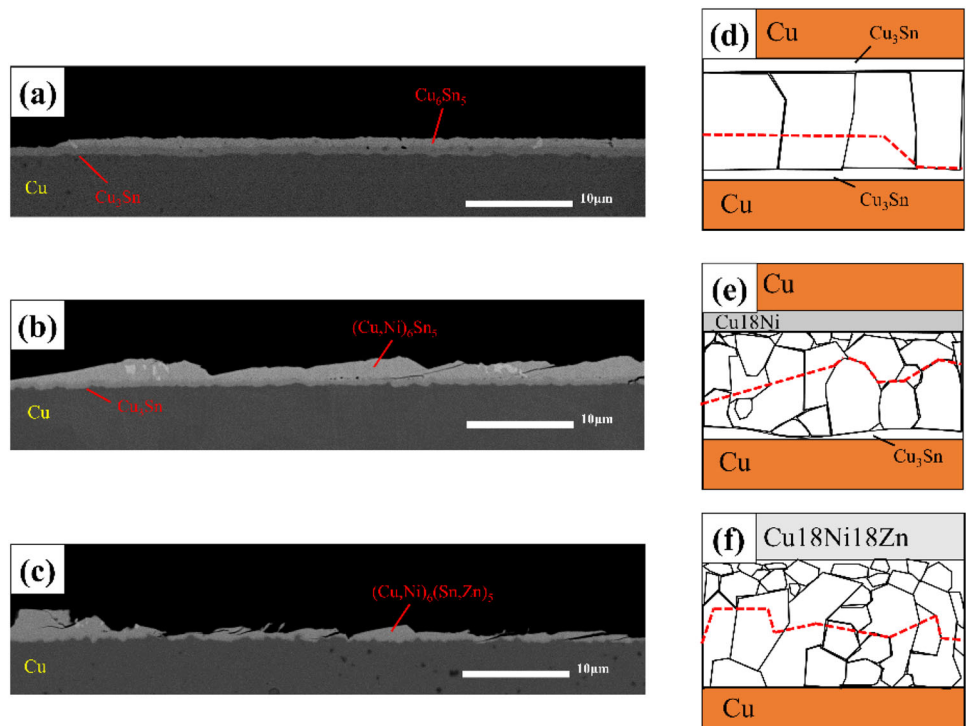
thicker planar Cu_3Sn layer exhibits in the micro-bump, Cu_6Sn_5 and Cu_3Sn interfacial delamination would act as a considerable failure mode [1]. Hence, complicated crack paths and phase boundaries modification both contributed to the promotion of joint reliability.

4 Conclusion

Three types of microbumps, Cu/Sn3.5Ag/Cu, Cu18Ni/Sn3.5Ag/Cu, and Cu18Ni18Zn/Sn3.5Ag/Cu, were investigated in this study. As indicated in the result of shear test, both Cu18Ni/Sn3.5Ag/Cu and Cu18Ni18Zn/Sn3.5Ag/Cu demonstrated superior mechanical properties than Cu/Sn3.5Ag/Cu. The strengthening mechanism was mainly attributed to grain refinement and the reduction of Cu_6Sn_5 preferred orientation. In Cu18Ni/Sn3.5Ag/Cu, Ni could improve the issues induced in Cu/Sn3.5Ag/Cu, such as Cu_6Sn_5 large columnar grains and strongly preferred orientation along the c-axis. In Cu18Ni18Zn/Sn3.5Ag/Cu, Zn addition not only resolved the issues mentioned above, but also provided significant effect for fracture toughness enhancement. Consequently, both Ni and Zn were effectively utilized to modify the grain structure and improve the intrinsic mechanical properties of Cu_6Sn_5, thereby enhancing the mechanical performances of Cu/Sn3.5Ag/Cu TLP bonding. In the near future, it is expected that doping Ni and Zn in Cu substrates may become a potential approach for 3D-IC package.

Author contributions

ZYW: Conceptualization, Writing—original draft. TCW: Resources. YCW: Resources. RWS: Resources, Validation. SYT: Resources. JGD: Conceptualization, Project administration, Supervision, Writing—review & editing.

Data availability

We ensured that all data and materials as well as software application or custom code support their published claims and comply with field standards.

Declarations

Conflict of interest The authors declare that they have no known competing financial interests or personal relationships that could have appeared to influence the work reported in this paper.

References

1. S.F. Choudhury, L. Ladani, Local shear stress-strain response of Sn-3.5Ag/Cu solder joint with high fraction of intermetallic compounds: Experimental analysis. J. Alloy. Compd. **680**, 665–676 (2016)
2. C.-Y. Ho et al., Bump height confinement governed solder alloy hardening in Cu/SnAg/Ni and Cu/SnAgCu/Ni joint assemblies. J. Alloy. Compd. **600**, 199–203 (2014)
3. W.-Y. Chen, J.-G. Duh, Suppression of Cu3Sn layer and formation of multi-orientation IMCs during thermal aging in Cu/Sn–3.5Ag/Cu–15Zn transient liquid-phase bonding in novel 3D-IC technologies. Mater. Lett. **186**, 279–282 (2017)
4. W.-Y. Chen, R.-W. Song, J.-G. Duh, Grain structure modification of Cu-Sn IMCs by applying Cu-Zn UBM on transient liquid-phase bonding in novel 3D-IC technologies. Intermetallics **85**, 170–175 (2017)
5. P. Yao et al., Shear strength and fracture mechanism for full Cu-Sn IMCs solder joints with different Cu3Sn proportion and joints with conventional interfacial structure in electronic packaging. Solder. Surf. Mount Technol. **31**(1), 6–19 (2019)
6. A.M. Gusak, K.N. Tu, C. Chen, Extremely rapid grain growth in scallop-type Cu6Sn5 during solid–liquid interdiffusion reactions in micro-bump solder joints. Scripta Mater. **179**, 45–48 (2020)
7. D. Mu et al., Investigating the mechanical properties, creep and crack pattern of Cu6Sn5 and (Cu,Ni)6Sn5 on diverse crystal planes. Mater. Sci. Eng. **566**, 126–133 (2013)
8. D. Mu et al., Growth orientations and mechanical properties of Cu6Sn5 and (Cu,Ni)6Sn5 on poly-crystalline Cu. J. Alloy. Compd. **536**, 38–46 (2012)
9. C.-Y. Yu, W.-Y. Chen, J.-G. Duh, Improving the impact toughness of Sn–Ag–Cu/Cu–Zn Pb-free solder joints under

high speed shear testing. J. Alloy. Compd. **586**, 633–638 (2014)

10. X. Zhang et al., Effect of Ni addition to the Cu substrate on the interfacial reaction and IMC growth with Sn3.0Ag0.5Cu solder. Appl. Phys. A **124**(4), 315 (2018)

11. H.-K. Cheng et al., Interfacial reactions between Cu and SnAgCu solder doped with minor Ni. J. Alloy. Compd. **622**, 529–534 (2015)

12. G. Zeng et al., The influence of Ni and Zn additions on microstructure and phase transformations in Sn–0.7Cu/Cu solder joints. Acta Mater. **83**, 357–371 (2015)

13. C.-Y. Yu, W.-Y. Chen, J.-G. Duh, Suppressing the growth of Cu–Sn intermetallic compounds in Ni/Sn–Ag–Cu/Cu–Zn solder joints during thermal aging. Intermetallics **26**, 11–17 (2012)

14. G. Zeng et al., Effect of Zn, Au, and In on the polymorphic phase transformation in Cu6Sn5 intermetallics. J. Mater. Res. **27**(20), 2609–2614 (2012)

15. W.-Y. Chen, C.-Y. Yu, J.-G. Duh, Improving the shear strength of Sn–Ag–Cu–Ni/Cu–Zn solder joints via modifying the microstructure and phase stability of Cu–Sn intermetallic compounds. Intermetallics **54**, 181–186 (2014)

16. C.-Y. Yu et al., Effects of minor Ni doping on microstructural variationsand interfacial reactions in Cu/Sn-3.0Ag-0.5Cu-xNi/Au/Ni sandwich structures. J. Electron. Mater. **39**(12), 2544–2552 (2010)

17. J. Wu, C.R. Kao, J. Yang. Mechanical reliability assessment of Cu_6Sn_5 intermetallic compound and multilayer structures in Cu/Sn interconnects for 3D IC applications. In: 2019 IEEE 69th Electronic Components and Technology Conference (ECTC). 2019

18. D. Mu, H. Huang, K. Nogita, Anisotropic mechanical properties of Cu6Sn5 and (Cu, Ni)6Sn5. Mater. Lett. **86**, 46–49 (2012)

19. W.-Y. Chen et al., Growth orientation of Cu–Sn IMC in Cu/Sn–3.5Ag/Cu–xZn microbumps and Zn-doped solder joints. Mater. Lett. **134**, 184–186 (2014)

20. F. Gao, T. Takemoto, H. Nishikawa, Effects of Co and Ni addition on reactive diffusion between Sn–3.5Ag solder and Cu during soldering and annealing. Mater. Sci. Eng. **420**(1), 39–46 (2006)

21. Y.-C. Wang et al., Diversifying grain orientation and expediting 10 μm Cu/Sn/Cu TLP bonding process with Ni doping. J. Mater. Sci. **32**(2), 2639–2646 (2021)

22. J.-M. Song et al., Relationship between nanomechanical responses of interfacial intermetallic compound layers and impact reliability of solder joints. Nanomaterials **10**(8), 1456 (2020)

23. Y.M. Leong et al., Microstructure and mechanical properties of Sn–1.0Ag–0.5Cu solder with minor Zn additions. J. Mater. Sci. **30**(13), 11914–11922 (2019)

24. S. Chen, W. Zhou, P. Wu, Effect of Zn Additions on the Mechanical Properties of Cu6Sn5-Based IMCs: Theoretical and Experimental Investigations. J. Electron. Mater. **44**(10), 3920–3926 (2015)

25. W.-Y. Chen et al., Retarding the Cu–Sn and Ag–Sn intermetallic compounds by applying Cu–xZn alloy on microbump in novel 3D-IC technologies. J. Mater. Sci. **26**(4), 2357–2362 (2015)

26. L. Jiang, N. Chawla, Mechanical properties of Cu6Sn5 intermetallic by micropillar compression testing. Scripta Mater. **63**(5), 480–483 (2010)

27. T.-T. Chou et al., Enhancement of the mechanical strength of Sn-3.0Ag-0.5Cu/Ni joints via doping minor Ni into solder alloy. Mater. Lett. **235**, 180–183 (2019)